Direct-Write Printed Current Sensor for Load Monitoring Applications

Yongchao Yu
Mechanical, Aerospace, and Biomedical Engineering
University of Tennessee
Knoxville, TN, USA
yyu6@utk.edu

Aravind K. Mikkilineni
Electrical and Electronics Systems Research Division
Oak Ridge National Laboratory
Oak Ridge, TN, USA
a.k.m@ieee.org

Stephen M. Killough
Electrical and Electronics Systems Research Division
Oak Ridge National Laboratory
Oak Ridge, TN, USA
killoughsm@ornl.gov

Teja Kuruganti
Computational Sciences and Engineering Division
Oak Ridge National Laboratory
Oak Ridge, TN, USA
kurugantipv@ornl.gov

Pooran C. Joshi
Electrical and Electronics Systems Research Division
Oak Ridge National Laboratory
Oak Ridge, TN, USA
joshipc@ornl.gov

Anming Hu
Mechanical, Aerospace, and Biomedical Engineering
University of Tennessee
Knoxville, TN, USA
ahu3@utk.edu

***Abstract*—We report on a flexible current sensor development employing direct-write printing and additive manufacturing techniques. The integrated current sensor unit incorporates sensing, data processing & storage, and in-field calibration capabilities. A combination of direct-write printing technique and low-temperature curable metallic ink is used to print Ag wires around a 12.5-µm-thick permalloy film. The overall thickness of the polyimide substrate and permalloy sheet remains well-below 500 µm enabling wrap-around sensor functionality. Fused deposition modeling (FDM) additive manufacturing is used to build custom parts for sensor mounting, encapsulation, and an in-field calibration unit using heat and chemical-resistant thermoplastic which responds well to mechanical stress. In the present configuration, the integrated current sensor unit can be powered through USB or 4 AAA batteries to allow data collection and sensor calibration in the field. The flexible current sensor employing a continuous sheet of the permalloy exhibited a well-behaved signal output response at peak current levels exceeding 15A and in the applied ac frequency range of 60 Hz – 10 kHz. Overall, the combination of direct-write printing, thin permalloy material, and additive manufacturing technique shows promise for the development of a reconfigurable low-cost current sensor that can be deployed in large numbers at locations of interest to avail the cost and energy-saving opportunities in industrial/commercial and residential applications.**

Keywords—printed sensor, flexible electronics, current sensor, additive manufacturing

I. Introduction

New technologies and approaches that are also low-cost are required to successfully exploit the full potential of end-use building loads for energy efficiency and grid services. Advanced sensors and controls can reduce the energy consumption of buildings by 20–40%, representing 0.3–0.4 quad in total energy savings when deployed on existing small and medium-size buildings [1]. Significant portions of building loads are dispatchable, and savings of several billion dollars in energy costs are projected with 10% participation in demand dispatch, enabling transactive energy. With buildings contributing 80% of the load growth through 2040, novel sensors and control technologies for buildings will play a significant role in grid modernization. As highlighted in Fig. 1, low-cost sensors are required for enhanced control of smart building loads and enable distributed energy resources to be "grid friendly." These advanced sensor platforms will not only enable monitoring and efficient control of building HVAC electrical loads, but also find applications in other market segments such as vehicle systems and distributed energy resources.

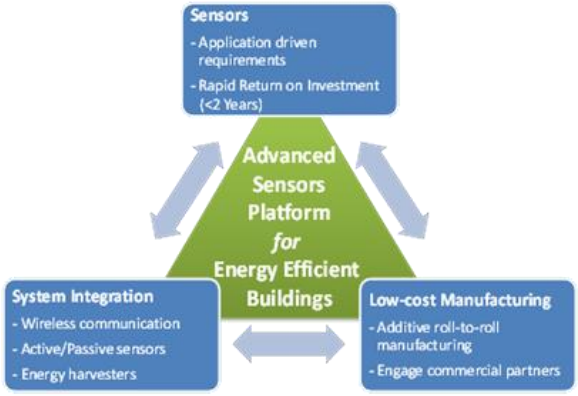

Fig. 1. Advanced sensor platform elements for grid-interactive smart building.

Advanced real-time load and power monitoring techniques are essential to establish a path towards grid-interactive smart building. Precise direct current (dc) and alternating current (ac) current measurements are fundamental for efficient power system instrumentation in diverse technology sectors such as automotive, buildings technology, chemical engineering, semiconductor industry, nuclear fusion, renewable energy, and consumer electronics. Techniques based on fundamental principles that lead to inherent electrical isolation, geometrical

XXX-X-XXXX-XXXX-X/XX/$XX.00 ©20XX IEEE

selectivity, and protection against large voltage/current transients are required for advanced current sensing applications. The basic parameters of any current sensor are linearity, offset, sensitivity, operating bandwidth, offset stability, and temperature/time sensitivity. Low-cost and high environmental resistance is a must for smart grid and industrial/residential applications. In the present work, we report on the design and development of a low-cost flexible current sensor and an integrated sensor unit employing a direct-write printing system, thin films of high permeability permalloy, and additive manufacturing technique. The emerging direct-write printing techniques, as shown in Fig. 2, offer large-scale processing and high throughput additive processing of a broad range of functional materials at high resolution to meet the cost, performance, and integration requirements for practical applications.

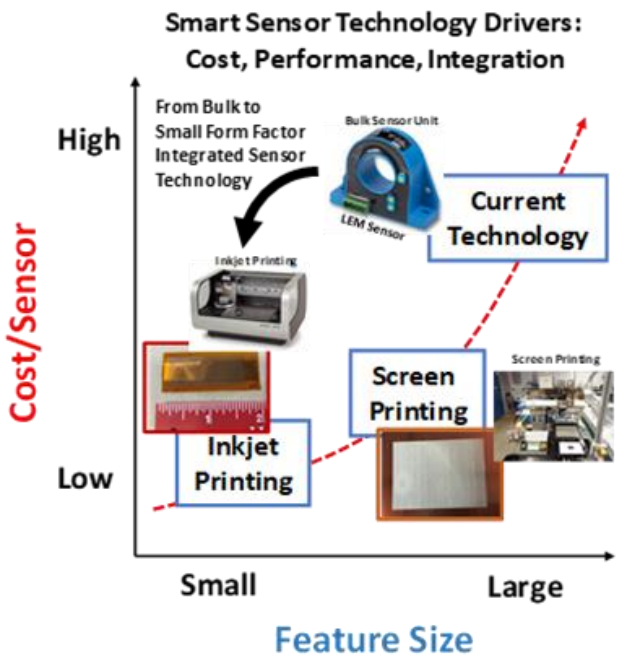

Fig. 2. Development of a printed current sensor meeting the cost, performance, and manufacturing demands for load-monitoring applications in building and smart grid.

II. Direct-write printed Sensor development

A. *Printed Current Sensor*

Fig. 3 (a) shows a CAD model of a sensing coil. The outer dimensions of this coil are 82 mm x 32 mm, with two electrical contacts on each end. The turn density of the coil (shown in silver) is 2.6 mm per turn with a trace width of 400 μm.

To create the coil, the silver (Ag) trace was printed on one side of a sheet of polyamide substrate. The silver trace was printed using an Optomec AJ200 aerosol jet printing system with CLARIANT Ag nanoparticle ink [2]. This system offers two methods for fine structure printing, a pneumatic atomizer (PA) and ultrasonic atomizer (UA). For this work the ultrasonic atomizer was used since it requires less ink volume than PA.

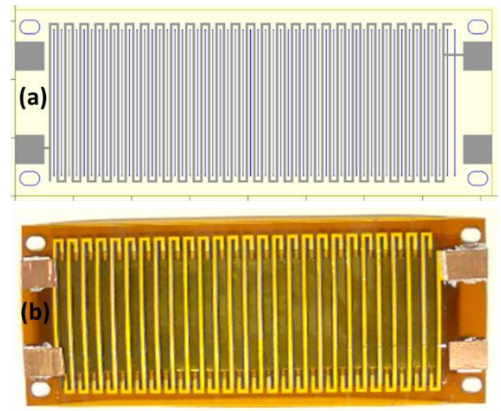

Fig. 3. Schematic of sensor coil design (a) and printed sensor (b).

The UA method functions by first atomizing liquid ink into aerosol droplets with diameters of 2-3 µm using high-frequency pressure waves generated by an ultrasonic transducer. The atomized ink droplets are then carried by a transport gas (nitrogen) from the ink vial to a deposition head. At the deposition head, a sheath gas focuses the aerosol and reshapes it into a narrow spray [2]. Typically for fine structure printing the line width can be adjusted between 10 μm – 100 μm using different combinations of nozzle sizes and sheath gas pressures. In this is work, silver coils were printed with 80 μm line width and 35% overlap. After printing, the coils were cured at 250 °C for 30 minutes to improve the overall conductivity of the printed trace [3,4].

Reduction in trace resistance can be achieved by printing multiple layers on top of each other. As the number of layers increase from 1 to 4, the thickness of the printed silver increases from about 1.5 μm to 5.5 μm (Fig.4(a)). As the number of layers are increased the trace resistance drops as shown in Fig.4(b), however additional layers beyond the third impart minimal conductivity gains. To balance reduction of trace resistance with time and cost of the printing process, the coils were printed using 3 layers of ink.

After printing, a layer of polyamide adhesive backed tape is placed on top of the printed layer as a protective film, avoiding covering the electrical contacts near the ends. A laser cutter is then used to make 100 μm wide cuts along the blue lines shown in Fig. 3 (a), ignoring any extra vertical cuts such as the two right-most ones. Note that the vertical cuts end with circular reliefs to prevent tearing of the polyamide material. The specific laser cutter used is an Epilog Zing 16, and which has a $16" \times 12"$ engraving/cutting area with a 30-watt CO_2 laser and 1000 dpi resolution.

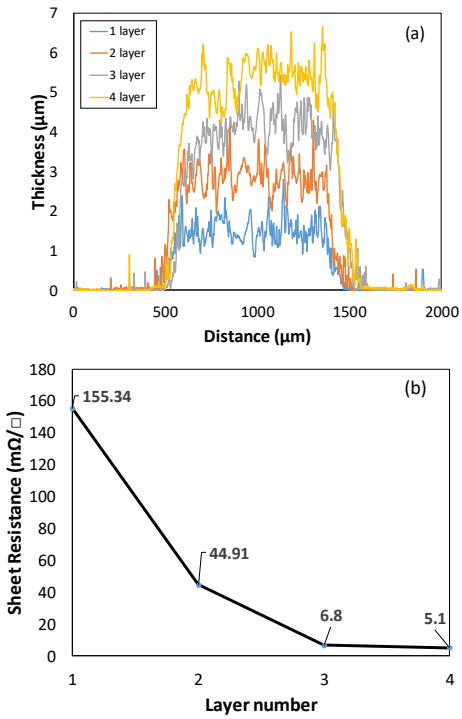

Fig. 4. (a）Thickness and（b）resistance measurement of printed Ag lines with different layer numbers.

Next a polyamide encased permalloy strip is woven through the vertical cuts such that the silver trace forms a coil around the strip as shown in Fig. 5. A tapered leader is attached to one end of the permalloy strip to ease the weaving process. Finally, the permalloy material is trimmed to minimize overlap and copper tape is attached to the electrical contacts using silver epoxy. The additional copper provides reinforcement where clamping force will be applied when in use. The combination of an improved silver printing process, polyamide protection layer of the silver and encapsulation of the core material, along with the copper contact reinforcements make this sense coil robust to handling stresses.

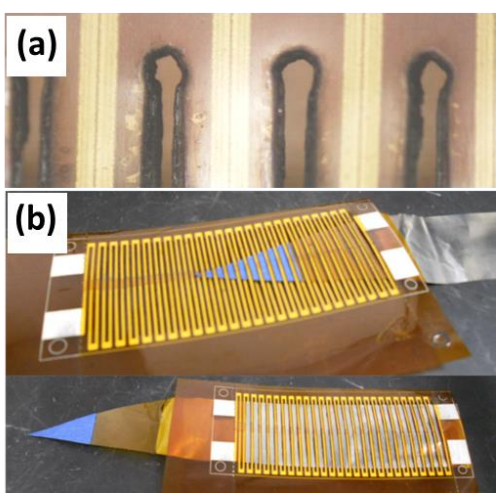

Fig. 5. Image of laser cuts (a) and permalloy strip being woven through the cuts (b).

B. *Sensor Integration*

A test fixture is used to attach the coil onto a current carrying conductor as illustrated in Fig. 6. This fixture was designed using SolidWorks CAD software and was created via fused deposition (FDM) of ABS with a Stratasys Dimension Elite 3D Printer. This printer is also used to create the electronics enclosure and external current loop described in later sections.

Installation of the printed sensor for current measurement is performed as follows. First the test fixture is attached to the conductor using an appropriately sized inner cross member as shown in the left-most column of images. Next one end of the sense coil is placed over the two alignment pips on the test fixture. The coil is wrapped around the test fixture and is held in place with a coil clamp which also provides an electrical connection to the coil. Finally, the coil and test fixture assembly are enclosed in a clamshell-like outer cover to prevent accidental contact with the exposed contacts (necessary in some high-voltage installations). The other end of the jacketed cable attached to the coil clamp can then be brought away from the potentially unsafe high-voltage area to be plugged into the current measurement electronics. Shielded Cat 5e ethernet cable has being used with all but one of the twisted pairs left unconnected.

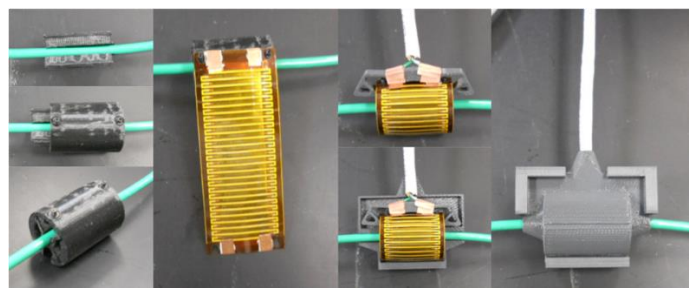

Fig. 4. Test fixture for installation of the sense coil around a current carrying wire.

C. *Measurement Electronics (may swap with (B) above)*

Electronics were designed to allow ease of development and testing of various coil designs and sensing algorithms, as well as to allow data collection in the field. The key components of this system are a low-noise high-gain analog front-end and an arbitrary signal generator for in-field coil calibration. These are centered around an ARM Cortex-M4 microcontroller (Teensy 3.2). A microSD card slot is provided for data collection, and a keypad and display facilitate user interaction while showing real-time measurement data. The unit can be powered externally through USB or internally with 4 AAA batteries, and uses a coin-cell battery to maintain its internal real-time clock.

The assembled electronics are shown in Fig. 7, which together with a battery holder are enclosed in a 3D printed case. On the front of the case are the keypad and display. On the right side from top to bottom is a connector for the sense coil, micro USB connector for power and data, and a small recessed switch to select between battery or USB power. On the top is a connector for an external current loop for sense coil calibration, and on the left is a microSD card slot. The back has a battery cover underneath which is a 4x AAA cell holder.

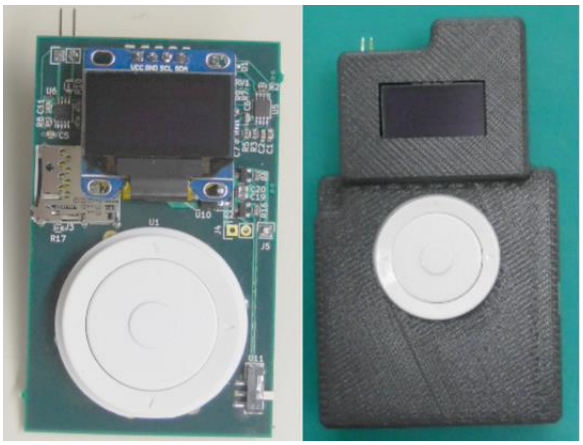

Fig. 5. Prototype hardware.

The typical response of each current sensor is on the order of 10 $\mu V/A$. In order to be effectively sampled by the ADC available in the selected microcontroller it is necessary for this signal to be amplified by a factor of 1000 or more. The specific implementation for this prototype hardware starts with a low-noise instrumentation amplifier (INA827) with a gain of 1000. The pre-amplified signal is then low-pass filtered using a 4th order Chebyshev filter with 5 kHz cutoff and is finally passed through a programmable-gain amplifier (PGA) to allow an additional gain between 1 and 32.

The amplified signal is sampled using the microcontroller's built-in 16-bit ADC at 44.1 ksps and low-pass filtered using a 500 Hz cutoff biquad filter before being analyzed. The fundamental frequency of the sampled signal is determined using the YIN algorithm [5] which can be implemented relatively efficiently with low-latency. Standard summation methods are used to estimate the RMS and peak amplitudes of the signal.

For in-field calibration and testing of sense coils, a signal generator is used to drive a multi-turn current loop (**Error! Reference source not found.**), allowing aggregate currents of up to several amps to be generated. The signal itself is generated by the microcontroller which outputs an analog signal using one of its internal digital-to-analog converters (DACs) which drives the LM4871 audio amplifier shown in the schematic. The output of the audio amplifier is brought out to a pin header to which an external current loop can connect. The external current loop is designed to allow the sense coil test fixture to directly mount onto it.

This configuration allows any arbitrary signal to be generated, not only sinusoidal ones, which can be useful when characterizing the transient or harmonic response of the sense coils. To ensure that a known current is passing through the current loop, a sense resistor is placed inline with the current loop and the voltage across it is amplified and sampled by the microcontroller. Knowledge of the actual current allows the signal sent to the DAC to be modified to compensate for changes in power supply voltage or variations between external current loops due to manufacturing tolerances or design changes.

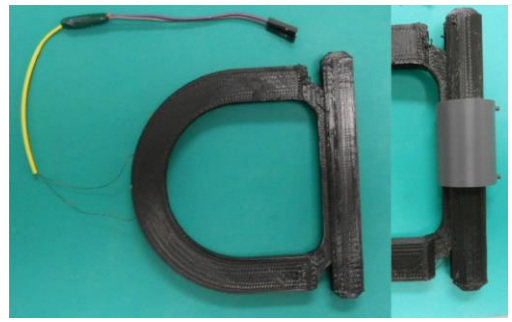

Fig. 6. Prototype external current loop for in-field coil calibration, consisting of 80 turns of magnet wire wound around a 3D printed form. The sense coil test fixture is able to slide directly onto the loop for testing.

A microSD card slot is included in the hardware for data storage, including both data collection as well as configuration storage. Each sense coil potentially has a different sensitivity, and may each require unique correction curves. While in operation, the measured data can be periodically written to the microSD card allowing stand-alone data collection. The written data includes the estimated frequency, current, amplifier gain setting, as well as a timestamp indicating when the measurement was obtained.

III. Sensor Performance

The theoretical response of the sense coil assuming a continuous cure with no gap can be derived directly from basic electromagnetic field theory which states that the voltage induced across the coil will be proportional to the time rate of change of magnetic flux, Φ, through the coil. This can be represented as

$$v_s = \frac{d\Phi}{dt} = \mu_c \rho A_c \frac{di}{dt} \qquad (V)$$

where v_s is the induced voltage, μ_c is the magnetic permeability of the permalloy (core material), A_c is the cross sectional area of the permalloy, ρ is the turn density of the printed coil, and i is the current in the conductor being measured. Note that the induced voltage increases proportionally with respect to the permeability and cross-sectional area of the core material, as well as the turn density of the sense coil. For a sinusoidal excitation current, the induced voltage also increases in proportion to the excitation frequency.

In reality there will always be a non-zero gap between the ends of the permalloy strip leading to the effective response shown below

$$v_s = \frac{d\Phi}{dt} = \mu_c A_c \frac{n}{l + \mu_{c,r} l_g} \frac{di}{dt} = \mu_c A_c \rho^\star \frac{di}{dt} \qquad (V)$$

where $\mu_c = \mu_{c,r}\mu_0$, l is the total length of the coil, and l_g is the length of the gap between the ends of the permalloy strip. The gap causes the effective turn density, ρ^*, to decrease as the gap length increases giving $\rho^* \leq \rho$. Using this model, a coil with length 8.5 cm, density of 3.3 mm/turn, and core permeability of 60000 with 10 µm gap would have a theoretical sensitivity of approximately 18 $\mu V/A$.

Another non-ideal behavior exhibited by the sensor is magnetic saturation of the permalloy. Many models for saturation have been developed, in particular the Jiles-Atherton model [6,7] is most commonly used and is approximated as

$$B_{eff} = B_{sat}\left(\coth\left(\frac{H}{a}\right) - \left(\frac{a}{H}\right)\right) \qquad (Wb/m^2)$$

where B_{eff} is the effective flux density, B_{sat} is the saturation point for magnetic flux density in the material, H is the applied magnetic field, and a is a scaling parameter experimentally selected as $B_{sat}/(4\mu_c)$. For simulation the ideal flux is first found to determine the magnetic field $H = \Phi/\mu_c A_c$, with which the effective flux $\Phi_{\text{eff}} = B_{eff}A_c$. The induced voltage then becomes $\text{v}_\text{s} = \text{d}\Phi_{\text{eff}}/dt$ which becomes strongly nonlinear as the current, and therefore induced magnetic field, increases.

Experimental results appear to be in line with the theoretical model. Several coils that have been characterized have shown sensitivities of approximately 10 $\mu V/A$. Characterization of one of the printed coils was performed using a current loop around which the sense coil was wrapped around using the test fixture described earlier. A commercial current transformer and oscilloscope were used to obtain ground-truth measurements of the actual current through the current loop. As shown in Fig. 7 the estimated current using the coil's response appears to be relatively linear for low currents, eventually deviating as the core begins to enter saturation. However, the relationship extending into the early saturation region can be modeled using a 3rd order polynomial as shown by the dashed red line in the figure.

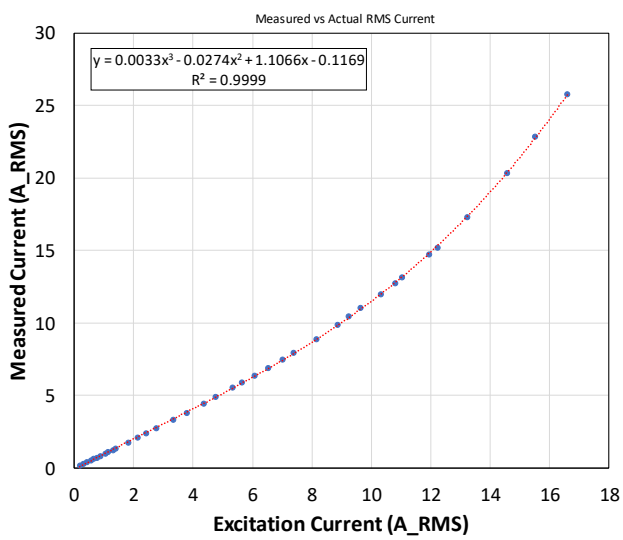

Fig. 7. Measured response from a printed sense coil using prototype measurement electronics showing near-linear behavior with a good 3rd order fit.

IV. CONCLUSIONS AND FUTURE WORK

The design and electrical performance of the direct-write printed flexible current sensor show promise for load monitoring applications in industrial/commercial and residential applications. Key findings of modeling, simulation, and analysis of the integrated current sensor align well with experimental results, and are guiding the integration of direct-write printing, additive manufacturing, and sensor electronics concepts to design a low-cost, reconfigurable field portable current sensor unit. Future modeling work will focus on extending the current sensing range through design modifications that are compatible with the direct-write printing and additive manufacturing approaches critical to meet the low-cost requirement for widespread deployment in buildings and grid applications.

ACKNOWLEDGMENT

This manuscript has been authored by UT-Battelle, LLC under Contract No. DE-AC05-00OR22725 with the U.S. Department of Energy. This material is based upon work supported by the U.S. Department of Energy, Office of Energy Efficiency and Renewable Energy. The United States Government retains and the publisher, by accepting the article for publication, acknowledges that the United States Government retains a non-exclusive, paid-up, irrevocable, world-wide license to publish or reproduce the published form of this manuscript, or allow others to do so, for United States Government purposes. The Department of Energy will provide public access to these results of federally sponsored research in accordance with the DOE Public Access Plan (http://energy.gov/downloads/doe-public-access-plan).

REFERENCES

[1] S. Katipamula, R. M. Underhill, J. K. Goddard, D. J. Taasevigen, M. A. Piette, J. Granderson, R. E. Brown, S. M. Lanzisera, and T. Kuruganti. 2012. Small- and Medium-Sized Commercial Building Monitoring and Controls Needs: A Scoping Study. PNNL-22169, Pacific Northwest National Laboratory, Richland, WA.

[2] M. E. Morales-Rodriguez, P. C. Joshi, J. R. Humphries, P. L. Fuhr, and T. J. Mcintyre, "Fabrication of Low Cost Surface Acoustic Wave Sensors Using Direct Printing by Aerosol Inkjet," *IEEE Access*, vol. 66, pp. 20907-20915, 2018.

[3] P. C. Joshi, T. Kuruganti, and S. M. Killough, "Impact of pulse thermal processing on the properties of inkjet printed metal and flexible sensors," ECS Journal of Solid State Science and Technology vol. 4, no. 4, Mar. 2015.

[4] T. Seifert, E. Sowade, F. Roscher, M. Wiemer, T. Gessner, and R. R. Baumann, "Additive manufacturing technologies compared: morphology of deposits of silver ink using inkjet and aerosol jet printing," Industrial & Engineering Chemistry Research, vol. 54, no. 2, pp. 769-779, 2015.

[5] A. De Cheveigné and H. Kawahara, "YIN, a fundamental frequency estimator for speech and music," *Journal of the Acoustical Society of America*, vol. 111 (4), pp. 1917-1930, April 2002.

[6] D. C. Jiles and D. L. Atherton, "Theory of ferromagnetic hysteresis," *Journal of magnetism and magnetic materials*, vol. 61, no. 1-2, pp. 48-60, 1986.

[7] F. Liorzou, B. Phelps, and D. L. Atherton, "Macroscopic models of magnetization," IEEE Transactions on Magnetics, vol. 36, no. 2, pp. 418-428, 2000.